Nonlinear Control of a Permanent Magnet Synchronous Wind Generator

R.D. Fernández
National University of Patagonia
San Juan Bosco
Comodoro Rivadavia, Argentina
CONICET
Email: dfernandez@unpata.edu.ar

F. Valenciaga
National University of La Plata
La Plata, Argentina
CONICET

R.R. Peña
National University of Patagonia
San Juan Bosco
Comodoro Rivadavia, Argentina
CONICET

***Abstract*—This work presents a nonlinear control of a wind generator equipped with a Permanent Magnet Synchronous Generator (PMSG). Three SISO controllers are developed, a Passivity based controller for the PMSG and its converter, and two Lyapunov controllers for the DC link and for the grid side converter, respectively. A general Control Strategy is presented in order to pass severe faults as symmetrical grid voltage dips. The proposed controllers are tested under realistic wind conditions.**

I. INTRODUCTION

It is well known that grid codes are becoming increasingly demanding of the wind farms with respect to voltage control, reactive range capability, active frequency control, etc [1][2]. In general this codes consider that wind generation must present similar operational characteristics to those of the conventional power plants [3][4].

Variable speed wind energy conversion systems (WECS) based on multipole permanent magnet synchronous generators (PMSG) is one of the most widespread configurations used around the world characterized by the mechanical robustness of PMSGs and by the absence of slips rings and gearbox, that simultaneously allows reducing the overall maintenance costs [5].

Following these general guidelines, the proposed control strategy presents a compound set of objectives selected according to the grid operation conditions (normal operation or presence of grid failures). In the first case, the multiple control objectives are to regulate the active and reactive power generated by the system in order to follow the references determined by the grid operator and also to maintain the voltage level on the DC bus. In case of grid faults (three voltage dips) the considered control structure allows preserving internal variables avoiding instabilities and large currents on the grid converter.

To fulfill control objectives the proposed control is designed through nonlinear techniques, Lyapunov [6][7] and Power Shaping Control [8][9] both of them well known because of their robustness properties.

II. DYNAMIC MODEL OF THE WECS

The WECS considered in this work is depicted in Figure 1.

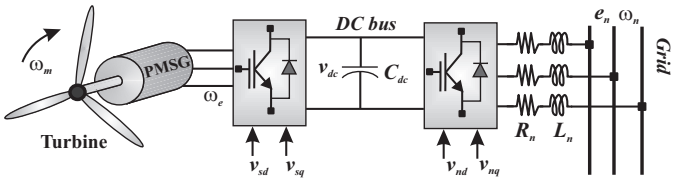

Fig. 1. Wind energy conversion system equipped with PMSG and full converters

The equations that describe the WECS dynamics can be written as [10]:

$$\dot{i}_{sd} = \left(-R_s i_{sd} + \omega_e L_{sq} i_{sq} - v_{sd}\right)/L_{sd} \quad (1)$$

$$\dot{i}_{sq} = \left(-R_s i_{sq} - \omega_e L_{sd} i_{sd} + \omega_e \Phi_{PM} - v_{sq}\right)/L_{sq} \quad (2)$$

$$\dot{\omega}_e = \frac{P}{2}\left(T_t(\omega_e,\nu) - \frac{3}{2}\frac{P}{2}\Phi_{PM} i_{sq}\right)/J \quad (3)$$

$$P_g = \frac{3}{2}\left(v_{sd} i_{sd} + v_{sq} i_{sq}\right) \qquad Q_g = \frac{3}{2}\left(v_{sq} i_{sd} - v_{sd} i_{sq}\right) \quad (4)$$

$$\dot{i}_{nd} = \left(-R_n i_{nd} + \omega_n L_n i_{nq} + v_{nd} - e_{nd}\right)/L_n \quad (5)$$

$$\dot{i}_{nq} = \left(-R_n i_{nq} - \omega_n L_n i_{nd} + v_{nq}\right)/L_n \quad (6)$$

$$P_n = \frac{3}{2} e_{nd} i_{nd}, \qquad Q_n = \frac{3}{2} e_{nd} i_{nq} \quad (7)$$

$$\dot{v}_{dc} = \frac{3\left(\left(v_{sd} i_{sd} + v_{sq} i_{sq}\right) - \left(v_{nd} i_{nd} + v_{nq} i_{nq}\right)\right)}{2 v_{dc} C_{dc}} \quad (8)$$

where i are currents, v and e voltages, P active power, Q reactive power, ω_e is the electrical angular frequency of the PMSG and R and L are resistances and inductances, respectively, Φ_{PM} is the magnetic rotor flux, P are the total poles number and J the inertia moment of the rotating parts. About subscripts, meanwhile s, n and DC indicate stator, grid variables and DC link ines, d and q indicate direct and quadrature axis according to the chosen reference frame. The PMSG reference frame is aligned with the rotor flux and at the grid connection side the reference frame is aligned with the line voltage spatial vector $e = e_{nd}$.

Thus, the dynamic behavior of this WECS can be described by the nonlinear model (1) - (8) with four control inputs v_{sd},

v_{sq}, v_{nd} and v_{nq}, two of them acting at the generator side inverter and the other ones at the grid side inverter and four outputs, currents at both sides, generator and grid ones.

Finally, P_t and T_t are wind turbine power and torque which depend on speed $\omega_m = 2\omega_e/P$ and wind velocity ν as:

$$P_t(\omega_e, \nu) = T_t\ \omega_m = \frac{1}{2}\rho A C_p \nu^3 \tag{9}$$

with ρ the air density, A the blade swept area and C_p the power coefficient which is a measure of turbine efficiency. C_p is usually presented as a function of the tip speed ratio $\lambda = R\omega_m/\nu$ (R is the radius) and the pitch blade angle β, $C_p(\lambda, \beta)$ [11] which depends on the turbine physical parameters.

III. Control Strategy and Control Techniques

The wind turbine control strategy employed in this work can be summarized as follows:

1) Normal Operation ($\gamma = 1$). Control objectives:
   a) Generator side: maximizing wind energy conversion (or other reference according to the Wind Farm Operator) and reactive neutral.
   b) Grid side: keeping DC link voltage constant and, about reactive power, neutral to the grid (or other).
2) Abnormal Operation ($\gamma = 0$, three phase voltage dips):
   a) Generator side: maintaining the DC bus voltage (expression (8)) and reactive neutral.
   b) Grid side: delivering as much as active power is possible and reactive neutral to the grid (or other).

Then, control strategy changes objectives according to an auxiliary parameter γ which reflects the grid state.

$$\gamma = \begin{cases} 0 & if \quad |e_n| \leq 0.85 \quad p.u. \\ 1 & if \quad 0.85 < |e_n| \leq 1.2 \quad p.u. \end{cases} \tag{10}$$

Figure 2 shows a block diagram of the system in the active power frame with SGC : the synchronous generator control, GCC: the grid converter control and DCC: the DC link control. The key point of the control strategy lies on the active power management by regulating the DC link voltage (enclosed in dashed lines in Figure 2) whose imbalance respect to the DC voltage reference is used to adjust other control loops according to γ. Figure 2 shows control paths for normal ($\gamma = 1$ and I in Figure 2) and abnormal ($\gamma = 0$ and II in Figure 2) operating conditions.

In this work, and according to (1) - (8), a state space description is used:

$$\dot{x} = f(x) + g(x)u \tag{11}$$
$$y = h(x) \tag{12}$$

with $x = [i_{sd}\ i_{sq}\ \omega_e\ v_{dc}\ i_{nd}\ i_{nq}]'$ and u, $g(x)$ and $h(x)$ defined considering to the analysed stage.

IV. Control laws

As indicated, the control strategy changes which control regulates the DC link voltage according to γ. Hence, DC link and grid converter controls are firstly addressed via Lyapunov theory and, finally, the PMSG control with Passivity.

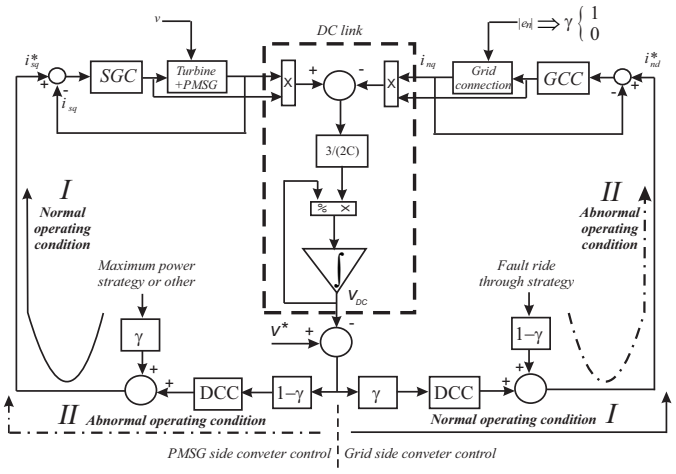

Fig. 2. Active power control strategy

A. DC link and grid side inverter controls

1) DC link Control: By remembering that the DC link voltage will be controlled by the grid side converter or the generator side one according to the parameter γ, control effort will be the stator current or the grid side converter current. In this way, if from the DC link voltage level (expression (8)), the reference frames are changed at both sides of the DC link ($v_{sd}^{'} = 0$ and $v_{nq}^{''} = 0$ at the generator side and at the grid side, respectively) simpler expressions appear:

$$\begin{aligned} \dot{x}_4 &= \frac{3v_{sq}^{'}i_{sq}^{'}}{2x_4C_{dc}} - \frac{3v_{nd}^{''}i_{nd}^{''}}{2x_4C_{dc}} = g_{1dc}u_1 - g_{2dc}u_2 \\ \dot{x}_a &= x_4^* - x_4 \end{aligned}$$

where control effort u_1 and u_2 (which are not performing simultaneously) are $i_{sq}^{'}$ and $i_{nd}^{''}$, respectively, but also an integration term in order to eliminate steady state errors is included.

The following Lyapunov function is proposed ($K_a > 0$):

$$V = \frac{1}{2}\left(\left(x_4^* - x_4\right)^2 + K_a\left(x_a^* - x_a\right)^2\right) \tag{13}$$

and by taking $\dot{V} \leq 0$ the next control laws are obtained:

$$u_2 = \frac{-1}{g_{2dc}}\left(K_{dc}\left(x_4^* - x_4\right) + K_a\int\left(x_4^* - x_4\right)dt - g_{1dc}i_{sq}^{'}\right)$$

$$u_1 = \frac{1}{g_{1dc}}\left(K_{dc}\left(x_4^* - x_4\right) + K_a\int\left(x_4^* - x_4\right)dt + g_{2dc}i_{nd}^{''}\right)$$

according to $\gamma = 1$ and $\gamma = 0$, respectively.

Note that, due to g_{1dc} and g_{2dc} are non linear functions of x_4, control laws are PI plus feedforward corrections.

2) Grid Side Inverter Control: Rewriting equations (5) and (6) and including integral control action on i_{nd} and i_{nq}, the grid side inverter dynamics can be expressed as:

$$\dot{x}_5 = \left(-R_n x_5 + \omega_n L_n x_6 + u_{nd} - e_{nd}\right)/L_n \tag{14}$$
$$\dot{x}_b = x_5^* - x_5 \tag{15}$$
$$\dot{x}_6 = \left(-R_n x_6 - \omega_n L_n x_5 + u_{nq}\right)/L_n \tag{16}$$
$$\dot{x}_c = x_6^* - x_6 \tag{17}$$

where x_5^* and x_6^* (i_{nd}^* and i_{nq}^*) are the references imposed by the Control Strategy. Even when there exist cross couplings between x_5^* and x_6^* in last expressions, active power depends exclusively on x_5 and reactive power depends on x_6 (expression (7)). Then, control laws are determined using a similar procedure to that one employed in the previous subsection. In this case, however, control actions are inverter voltages $u_{nd} = v_{nd}$ and $u_{nq} = v_{nq}$. Both control laws are derived via independent ways from the following two Lyapunov functions:

$$V_d = \frac{1}{2}\left(\left(x_5^* - x_5\right)^2 + K_{dI}\left(x_b^* - x_b\right)^2\right) \quad (18)$$

$$V_q = \frac{1}{2}\left(\left(x_6^* - x_6\right)^2 + K_{qI}\left(x_c^* - x_c\right)^2\right) \quad (19)$$

with $K_{dP} > 0$ and $K_{dQ} > 0$. Control actions are:

$$\begin{aligned} u_{nd} &= K_{dP}L_n\left(x_5^* - x_5\right) + K_{dI}L_n\int(x_5^* - x_5)dt + \\ &+ R_n x_5 - \omega_n L_n x_6 + e_{nd} \\ u_{nq} &= K_{dQ}L_n\left(x_6^* - x_6\right) + K_{qI}L_n\int(x_6^* - x_6)dt + \\ &+ R_n x_6 + \omega_n L_n x_5 \end{aligned}$$

B. Power shaping PMSG control

Beginning with the dynamical system defined in expressions (11) and (12) and according to [9]:

1) There exists a full rank matrix $Q : R^n \rightarrow R^{n\times n}$ that solves (Poincare's lemma):
   a) $\nabla(Qf) = \nabla(Qf)^T$
   b) $Q + Q^T \leq 0$
2) There exists a potential function $P_a : R^n \rightarrow R$ which:
   a) $g^{\perp}Q^{-1}\nabla P_a = 0$ with $g^{\perp}g = 0$
   b) $x_* = \arg\min P_d(x)$ where $P_d(x) = \int[Q(x)f(x)]^T dx + P_a(x)$
3) After verifying last conditions, the control action:

$$u = (g^T Q^T Q g)^{-1} g^T Q^T \nabla P_a \quad (20)$$

assures that x_* is a locally equilibrium point with Lyapunov function P_d. Additionally, according to LaSalle's theorem it is possible obtaining the domain of attraction of P_d. Due to constraint $(1.a)$ is difficult to verify, a modification over Q matrix can be employed [8]:

$$\tilde{Q} = \left[\frac{1}{2}\nabla(Qf)M + \frac{1}{2}\nabla^T(MQf) + \kappa I\right]Q \quad (21)$$

$$\tilde{P}_d(x) = \int[\tilde{Q}(x)f(x)]^T dx + P_a(x) \quad (22)$$

$$\tilde{g} = \tilde{Q}g. \quad (23)$$

The subsystem dynamics given by (1), (2) and (3) presents two control inputs, one of them ($u_{sd} = v_{sd}$) is used to nullify the reactive power on the PMSG terminals. Then, expression (4), this objective is fulfilled by $u_{sd} = u_{sq}\frac{x_1}{x_2}$. Carrying out the design procedure, the control law can be expressed as ($L_{sq} = L_{sd} = L_s$):

$$u_{sq} = -\frac{2K_4L_s x_2^2(x_2 - x_2^*)}{(x_1^2 + x_2^2)} - \frac{u_{sq}^* x_2\left(x_1\frac{x_1^*}{x_2^*} + x_2\right)}{(x_1^2 + x_2^2)}$$

the detailed procedure to determine this expression can be seen in the Appendix, and it can be approximated, close to the equilibrium point ($x \approx x^*$), by:

$$u_{sq} \approx -\frac{2K_4L_s x_2^2(x_2 - x_2^*)}{(x_1^2 + x_2^2)} - u_{sq}^*$$

Meanwhile the first term of this last nonlinear control expression is proportional to the error, the second part is the desired equilibrium point. On the other hand, because of model uncertainties, it is important to note the steady state error can be reduced by increasing K_4 or it can be eliminated including an integral state in the controller. In this way, the integral term $(K_{int}\int(i_{sq} - i_{sq}^*)dt)$ is added to the control law. Then, the final control law is:

$$u_{sq} = -\frac{2K_4L_s x_2^2(x_2 - x_2^*)}{(x_1^2 + x_2^2)} - u_{sq}^* - K_{int}\int(x_2 - x_2^*)dt$$

V. Simulation results

In order to analyze the performance of the proposed control this section shows the results of representative simulations. These studies where carried out using a 2MW PMSG whose parameters were taken from [12]. To test the system behavior, keeping wind speed constant, a sudden symmetrical three phase voltage drop of about 80% of the rated voltage and 1 second width [13, pp 20-21] was considered at $t = 60$s. Figure 3 depicts the time profiles corresponding to the control references and the DC link voltage level. According with the control purpose, these references are closely followed by the corresponding real system currents which are not shown in the figure. Regarding the figure, it is interesting to note that immediately after the voltage dip, the reference i_{nd}^* experiments a fast increasing of about a 25% with the objective of giving support to the utility net. Indeed, the Control Strategy maximises active power delivered by increasing i_{nd}^* to its maximum value. However, because of the voltage drop at the grid connection point, this current increment is not followed by a proportional active power deliver which actually decreases. The general control strategy and the controllers behavior show a very good performance which can be corroborated in the DC bus voltage profile depicted in Figure 3(c). Despite the strong variations of the currents references at the voltage dip edges, the DC bus experiments an overvoltage of about a 13%, with a fast recovering. It should be noted that the abrupt references changes are produced not only by the switching strategy, but also by the feedforward control actions used in the DC link controller. It is worth noting that due to reactive power behaviors at both ends, i.e. generator and grid sides, are neutral, in all of the carried out simulations, Q_g is identically zero because of, Subsection §IV-B, it is a consequence of an algebraic relation. About grid side, reactive power experiences a minor dynamics of unimportant value.

Figure 4 presents some variables in order to analyze the wind generator behavior under a real wind profile and employing the same the voltage dip. In order to emphasize the behavior close to the voltage dip, the wind velocity profile is

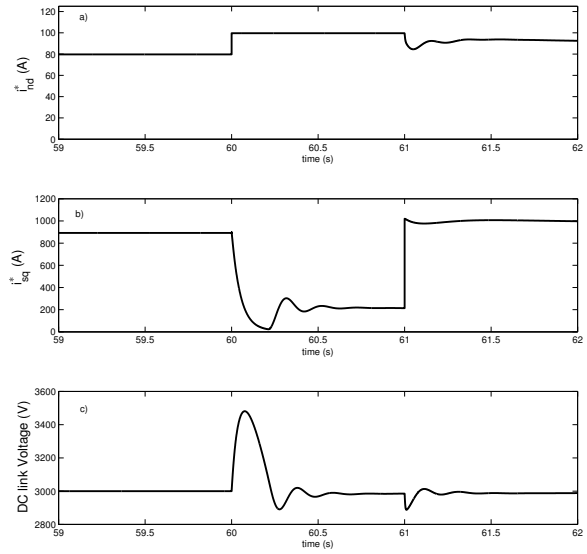

Fig. 3. i_{nd}, i_{sq} and V_{DC} behaviors under a symmetrical voltage drop. a) i_{nd} at the grid converter side, b) PMSG i_{sq} and c) DC link voltage V_{DC}

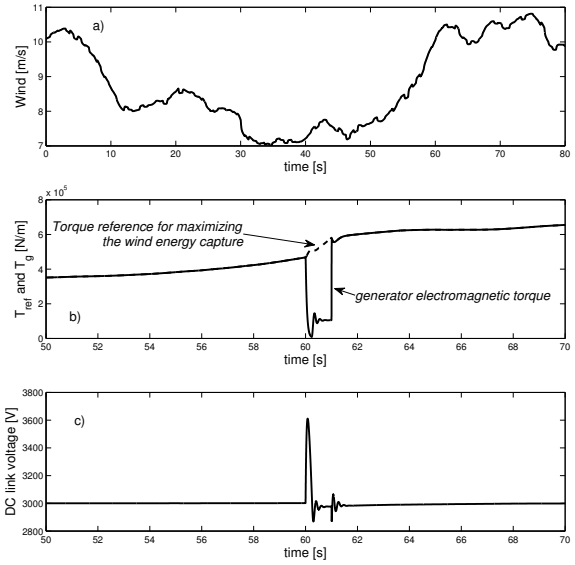

Fig. 4. Realistic wind and torques and DC link voltage behaviors under a symmetrical voltage drop. a) Real wind profile, b) Generator torque and optimum torque and c) DC link voltage

presented all of the time (Figure 4 (a)) but the other variables are indicated between 50 and 70 seconds.

In part (b) of Figure 4, the generator torque follows the reference one almost all the time except in the voltage dip. Indeed, because of the reference of the generator torque is built from maximizing the wind energy extraction, the generator controller copies the reference in such a way that under normal conditions it is ensured that the wind generator is delivering the maximum available power. Under abnormal operation, the reference of maximizing power lost importance and the Control Strategy switches the generator reference in order to pass the voltage dip. In this way, both torques reference and generator are different as indicated in part (b) of Figure 4. In part (c), the DC link voltage indicates that there is a transitory behavior of a short duration and with a maximum value of 20% of the nominal one. Active powers, generator and grid side ones, are not presented due to they present a similar (qualitative) behavior than the electromagnetic torque.

VI. CONCLUSIONS

A global strategy for operating WECS under severe symmetrical voltage faults was proposed. The overall Control Strategy was accomplished via three SISO controllers which were designed keeping in mind the nonlinear nature of the system but also the nonlinear structural change. In this way, meanwhile a nonlinear controller based on Power Shaping Passivity technique was proposed in order to drive the PMSG, the other two controllers were designed in the Lyapunov frame in order to ensure stability properties too.

Simulation results indicated good behaviours under demanding signal as a constant wind and a real wind profile both of them considering a severe symmetrical fault.

As a future work, further analysis to solve the control of the WECS as a MIMO system will allow to propose a multivariate controller under Passive framework. In the same way, distorted and imbalanced grid voltages will be considered.

APPENDIX

This appendix summarises steps which ensure the stability of the control action, expression (20), for the PMSG.

Because of original matrix $Q + Q^T >< 0$ in expressions (1), (2) and (3) then, applying (21), (22) and (23):

$$\tilde{Q} = \begin{pmatrix} \kappa & 0 & 0 \\ 0 & \kappa & 0 \\ 0 & 0 & \kappa \end{pmatrix} \text{ with } \kappa < 0$$

According to $g^{\perp}\tilde{Q}^{-1}\nabla P_a = 0$ with $g^{\perp}g = 0$:

$$\begin{aligned} P_a \quad &\rightarrow \quad \Phi(x_1, x_2) \Rightarrow P_a = K_1(x_1 - x_1^*) + \\ &+ \quad K_2(x_1 - x_1^*)^2 + K_3(x_2 - x_2^*) + K_4(x_2 - x_2^*)^2 \end{aligned}$$

Due to $x_* = \arg\min P_d(x)$ where $P_d(x) = \int [\tilde{Q}(x) f(x)]^T dx + P_a(x) \Rightarrow \nabla P_d(x_1, x_2, x_3)\Big|_{x=x^*} = 0$

$$\Rightarrow \nabla P_d(x_1, x_2, x_3)\Big|_{x=x^*} = 0$$

$$\left(\begin{array}{c} K_1 + 2K_2(x_1 - x_1^*) - \kappa \left(\frac{R_s x_1}{L_{sq}} - x_2 x_3 \right) \\ K_3 + 2K_4(x_2 - x_2^*) - \kappa \left(\frac{R_s x_2 + x_3(L_{sq} x_1 - \Phi_{PM})}{L_{sq}} \right) \\ \kappa \frac{P}{2} \left(T_t(x_3, \nu) - \frac{3}{2} \frac{P}{2} \Phi_{PM} x_2 \right) / J \end{array} \right) \Bigg|_{x=x^*}$$

$$\Rightarrow K_1 = \kappa\left(\frac{R_s x_1^*}{L_{sq}} - x_2^* x_3^*\right)$$
$$\Rightarrow K_3 = \kappa\left(\frac{R_s x_2^* + x_3^*(L_{sq}x_1^* - \Phi_{PM})}{L_{sq}}\right)$$
$$\Rightarrow T_t(x_3,\nu)\Big|_{x=x^*} = \frac{3}{2}\frac{P}{2}\Phi_{PM}x_2^*$$

and considering the Hessian condition

$$\nabla^2 P_d(x_1,x_2,x_3)\Big|_{x=x^*} > 0$$

$$\begin{pmatrix} 2K_2 - \frac{\kappa R_s}{L_{sq}} & \kappa x_3 & \kappa x_2 \\ -\kappa x_3 & 2K_4 - \frac{\kappa R_s}{L_{sq}} & \kappa\left(-x_1 + \frac{\Phi_{PM}}{L_{sq}}\right) \\ 0 & -\frac{3\kappa P^2 \Phi_{PM}}{8J} & \frac{\partial^2 P_d}{\partial x_3^2} \end{pmatrix} > 0$$

Note that $K_2 = 0$ and $K_4 > 0$ verify first two principal minor conditions according to Sylvester test provided that $\frac{\kappa R_s}{L_{sq}} < 0$. About the third condition $|\nabla^2 P_d|_{x=x^*} =$

$$\frac{3\kappa P^2\Phi_{PM}}{8J}\left(\kappa\left(-\frac{\kappa R_s}{L_{sq}}\right)\left(-x_1 + \frac{\Phi_{PM}}{L_{sq}}\right) + \kappa^2 x_2 x_3\right) + \\ + \frac{\partial^2 P_d}{\partial x_3^2}\left(\left(-\frac{\kappa R_s}{L_{sq}}\right)\left(2K_4 - \frac{\kappa R_s}{L_{sq}}\right) + \kappa^2 x_3^2\right) \quad (24)$$

It is important to note that meanwhile the first term of (24) is almost always positive, the second one is positive if $\frac{\partial^2 P_d}{\partial x_3^2} > 0$ and, then, by properly chosen K_4 stability can be assured.

In order to demonstrate that $\frac{\partial^2 P_d}{\partial x_3^2} > 0$ and beginning with the electrical torque in the low to nominal wind speed range, i.e. $\beta = 0$, it is well known that meanwhile $T_t(v, x_3, \beta) = T_t(v, x_3)$, the electrical torque T_e is driven to maximize extracted wind power, i.e. $T_e = \frac{3}{2}\frac{P}{2}\Phi_{PM}x_2 = k_{opt}x_3^2$ with $k_{opt} > 0$ a turbine dependent (known) parameter. Then, from expression (24):

$$\frac{\partial^2 P_d}{\partial x_3^2} = \frac{\kappa}{J}\frac{P}{2}\frac{\partial\left(T_t(x_3,\nu) - k_{opt}x_3^2\right)}{\partial x_3}$$
$$\frac{\partial^2 P_d}{\partial x_3^2} = \frac{\kappa}{J}\frac{P}{2}\left(\frac{\partial T_t(x_3,\nu)}{\partial x_3} - 2k_{opt}x_3\right)$$

And from (9)

$$T_t = \frac{1}{2}\frac{\rho A C_p \nu^3}{x_3} = \frac{kC_p\nu^3}{x_3}$$
$$\frac{\partial T_t}{\partial x_3} = \frac{k\nu^3\left(\partial C_p/\partial\lambda\right)\left(\partial\lambda/\partial x_3\right)x_3 - kC_p\nu^3}{x_3^2}$$
$$\frac{\partial^2 P_d}{\partial x_3^2} = \frac{\kappa}{J}\frac{P}{2}\left(\frac{k\nu^3\left(\partial C_p/\partial\lambda\right)\lambda - P_t - 2k_{opt}x_3^3}{x_3^2}\right) \quad (25)$$

As aforesaid, beginning with low and ending in nominal wind speed, tracking the optimum torque indicates extracting maximum power available in the wind in steady state which means, because the maximum is obtained, a maximum power coefficient $C_p = C_{pmax}$ and $\partial C_p/\partial\lambda = \partial C_{pmax}/\partial\lambda = 0$. Then, expression (25) becomes bigger than zero provided that $\kappa < 0$.

In the region delimited by nominal to maximum wind velocities, an item not covered in this work, in order to reduce turbine torque, pitch control drives β in such a way that stability of the wind turbine is ensured [14][15] keeping constant turbine velocity x_3 or another associated variable to x_3 as power [16]. This control law, obviously, must ensure $|\nabla^2 P_d|_{x=x^*} > 0$.

As a consequence, in both operation zones, i.e. tracking the optimum or in the upper wind zone, stability is ensured via the Hessian matrix.

REFERENCES

[1] C. Sourkounis and P. Tourou, "Grid code requirements for wind power integration in europe," *Conference Papers in Energy. Hindawi Publishing Corporation*, vol. 2013, 2013.

[2] K. Hemmes, "Towards multi-source multi-product and other integrated energy systems," *International Journal of Integrated Energy Systems*, vol. 1, no. 1, pp. 1–15, Jan-June 2009.

[3] M. Milligan, K. Porter, E. DeMeo, P. Denholm, H. Holttinen, B. Kirby, N. Miller, A. Mills, M. O'Malley, M. Schuerger, and L. Soder, "Wind power myths debunked," *IEEE Power & Energy Magazine*, no. 09, pp. 89–99, Nov-Dec 2009.

[4] J. Kabouris and F. Kanellos, "Impacts of large-scale wind penetration on designing and operation of electric power systems," *IEEE TRANSACTIONS ON SUSTAINABLE ENERGY*, vol. 1, no. 2, pp. 107–114, July 2010.

[5] A. Hansen and G. Michalke, "Modelling and control of variable-speed multi-pole permanet magnet synchronous generator wind turbine," *Wind Energy*, vol. 11(5), p. 537 554, 2008.

[6] H. Khalil, *Nonlinear Systems (2nd Edition)*. Pentice-Hall Inc., 1996.

[7] M. Haddad and V. Chellaboina, *Nonlinear Dynamical Systems and Control. A Lyapunov-Based Approach*. Princeton University Press, 2008.

[8] R. Ortega, D. Jeltsema, and J. Scherpen, "Power shaping: A new paradigm for stabilization of nonlinear rlc circuits," *IEEE TRANSACTIONS ON AUTOMATIC CONTROL*, vol. 48, no. 10, pp. 1762–1768, Oct 2003.

[9] E. García-Canseco, R. Ortega, J. Scherpen, and D. Jeltsema, *Power Shaping Control of Nonlinear Systems: A Benchmark Example in Lagrangian and Hamiltonian Methods for Nonlinear Control 2006*. Springer, 2007, vol. 366, ch. 10, pp. 135–146.

[10] K. Krause, *Electric Machines*. Prentice-Hall, 1986.

[11] A. Rolan, A. Luna, G. Vazquez, D. Aguilar, and G. Azevedo, "Modeling of a variable speed wind turbine with a permanent magnet synchronous generator," in *Proceedings of IEEE Int. Symp. on Ind. Elect.*, 2009.

[12] B. Wu, Y. Lang, N. Zargari, and S. Kouro, *Power Conversion and Control of Wind Energy Systems*, L. Hanzo, Ed. Wiley - IEEE Press, 2011.

[13] F. Iov, A. Hansen, P. Sørensen, and N. Cutululis, "Mapping of grid faults and grid codes," Risø National Laboratory Technical University of Denmark, Roskilde, Denmark, Report Risø-R-1617(EN), July 2007.

[14] F. Bianchi, H. De Battista, and R. Mantz, *Wind Turbine Control Systems. Principes, Modelling and Gain Scheduling*. Berlin Heidelberg: Springer, 2006.

[15] I. Munteanu, A. Bratcu, N. Cutululis, and E. Ceangă, *Optimal Control of Wind Energy Systems.Towards a Global Approach*. London: Springer, 2008.

[16] V. Akhmatov, "Anlysis of dynamic behviour of electric power systems with large amount of wind power," Ph.D. dissertation, Technical University of Denmark, Kgs. Lyngby, Denmark, April 2003.